Cerebellar ataxia and Purkinje cell dysfunction caused by Ca^{2+}-activated K^+ channel deficiency

M. Sausbier*†, H. Hu†‡, C. Arntz*, S. Feil§, S. Kamm§, H. Adelsberger¶, U. Sausbier*, C. A. Sailer‖, R. Feil§, F. Hofmann§, M. Korth**, M. J. Shipston††, H.-G. Knaus‖, D. P. Wolfer‡‡, C. M. Pedroarena§§, J. F. Storm‡¶¶, and P. Ruth*¶¶

*Pharmakologie und Toxikologie, Pharmazeutisches Institut, and §§Abteilung für Kognitive Neurologie, Hertie Institut für Klinische Hirnforschung, Universität Tübingen, D-72076 Tübingen, Germany; ‡Institute of Physiology and Centre for Molecular Biology and Neuroscience, University of Oslo, N-0317 Oslo, Norway; §Institut für Pharmakologie und Toxikologie, Technischen Universität München, D-80802 Munich, Germany; ¶Physiologisches Institut, Zelluläre Physiologie, Universität München, D-80336 Munich, Germany; ‖Institut für Biochemische Pharmakologie, Universität Innsbruck, A-6020 Innsbruck, Austria; **Institut für Pharmakologie für Pharmazeuten, Universitätsklinikum Hamburg–Eppendorf, D-20246 Hamburg, Germany; ††Membrane Biology Group, Division of Biomedical Science, University of Edinburgh Medical School, Edinburgh EH8 9XD, Scotland; and ‡‡Anatomisches Institut, Neuroanatomie und Verhalten, Universität Zürich, CH-8057 Zurich, Switzerland

Edited by Per O. Andersen, University of Oslo, Oslo, Norway, and approved May 11, 2004 (received for review March 12, 2004)

Malfunctions of potassium channels are increasingly implicated as causes of neurological disorders. However, the functional roles of the large-conductance voltage- and Ca^{2+}-activated K^+ channel (BK channel), a unique calcium, and voltage-activated potassium channel type have remained elusive. Here we report that mice lacking BK channels ($BK^{-/-}$) show cerebellar dysfunction in the form of abnormal conditioned eye-blink reflex, abnormal locomotion and pronounced deficiency in motor coordination, which are likely consequences of cerebellar learning deficiency. At the cellular level, the $BK^{-/-}$ mice showed a dramatic reduction in spontaneous activity of the $BK^{-/-}$ cerebellar Purkinje neurons, which generate the sole output of the cerebellar cortex and, in addition, enhanced short-term depression at the only output synapses of the cerebellar cortex, in the deep cerebellar nuclei. The impairing cellular effects caused by the lack of postsynaptic BK channels were found to be due to depolarization-induced inactivation of the action potential mechanism. These results identify previously unknown roles of potassium channels in mammalian cerebellar function and motor control. In addition, they provide a previously undescribed animal model of cerebellar ataxia.

Potassium channels are the largest and most diverse class of ion channels underlying electrical signaling in the brain (1). By causing highly regulated, time-dependent, and localized polarization of the cell membrane, the opening of K^+ channels mediates feedback control of excitability in a variety of cell types and conditions (1). Consequently, K^+ channel dysfunctions can cause a range of neurological disorders (2–6), and drugs that target K^+ channels hold promise for a variety of clinical applications (7).

Among the wide range of voltage- and calcium-gated K^+ channel types, one stands out as unique: the large-conductance voltage- and Ca^{2+}-activated K^+ channel (BK channel, also termed *Slo* or Maxi-K) differs from all other K^+ channels in that it can be activated by both intracellular Ca^{2+} ions and membrane depolarization (8). These channels are widely expressed in central and peripheral neurons, as well as in other tissues (9), and are regarded as a promising drug target (10). However, the functions of the BK channels *in vivo* have not previously been directly tested in any vertebrate species. We therefore decided to examine the functions of these channels by inactivating the gene encoding the pore-forming channel protein.

Methods

A complete description of the methods is given in *Supporting Methods*, which is published as supporting information on the PNAS web site.

Generation of BK Channel α Subunit-Deficient Mice. In the targeting vector (Fig. 5, which is published as supporting information on the PNAS web site), the pore exon was flanked by a single loxP site and a floxed *neo/tk* cassette. Correctly targeted embryonic stem cells were injected into C57BL/6 blastocysts and resulting chimeric mice mated with C57BL/6. Homozygous BK-deficient mice (F_2 generation) were produced. Either litter- or age-matched WT and $BK^{-/-}$ mice on a hybrid SV129/C57BL6 background (always F_2 generation) were randomly assigned to the experimental procedures, in keeping with German legislation on the protection of animals.

Brain *in Situ* Hybridization and Immunohistochemistry. BK channel α subunit mRNA transcript antisense probes complementary to the pore exon were labeled with [α-^{35}S]dATP to a specific activity of $\approx 10^9$ cpm/μg. Sections (15 μm) were cut on a cryostat and fixed in 4% paraformaldehyde. Sections were prehybridized with hybridization buffer containing yeast tRNA and salmon sperm DNA and exposed to labeled probe (5,000 cpm/μl) in hybridization buffer. Sections were washed and exposed for 28 days.

Immunhistochemistry was performed by using cryostat slices from perfused and postfixed brains. Coronal cerebellar were incubated with anti-BK$\alpha_{(674-1115)}$ tagged with a peroxidase-conjugated goat anti-rabbit IgG.

Motor Function, Motor Learning, and Footprint Patterns. For analyzing balance and motor coordination, 12 male and 12 female mice of each genotype (4–6 months) were tested on the accelerating rotarod (11); the rotational speed increased from 4 to 40 rpm over 5 min. Mice were trained for 3 days with five trials per day before latency to fall was recorded.

The ability of the mice to traverse a graded beam with smooth or irregular surface was assessed (12). Before testing, the mice were trained for 3 days with four trials per day.

Hindpaws and forepaws of six WT and seven $BK^{-/-}$ mice (litter- or age-matched, 3–6 months) were dipped in red and blue watercolor, respectively, before walking on paper (12). Mice were trained on 3 consecutive days with 3 trials per day. Footprint patterns were analyzed for stride basis, stride length, and paw abduction.

Conditioned Eye Blink. Eye-blink conditioning (13) from 8 WT and 8 $BK^{-/-}$ mice (8–12 weeks) was performed with a tone (5 kHz) as conditioned stimulus (CS) and an air puff (10 psi) as uncon-

This paper was submitted directly (Track II) to the PNAS office.

Abbreviations: BK channel, large-conductance voltage- and Ca^{2+}-activated K^+ channel; AHP, afterhyperpolarization; PC, Purkinje cell; AP, action potential; DCN, deep cerebellar nuclei; IbTx, iberiotoxin.

†M.S. and H.H. contributed equally to this work.

¶¶To whom correspondence may be addressed. E-mail: johan.storm@basalmed.uio.no or peter.ruth@uni-tuebingen.de.

www.pnas.org/cgi/doi/10.1073/pnas.0401702101

ditioned stimulus (US). The US was coterminated with the CS. Conditioning (each session consisting of 90 paired CS-US trials and 10 CS trials alone) was performed successively for 5 days and extinction (each session consisting of 20 CS alone) for 3 days.

Electrophysiological Analysis of Cerebellar Purkinje Cells (PCs). Sagittal slices (350–400 μm thick) from the cerebellar vermis of 4- to 5-week-old WT and BK$^{-/-}$ mice were prepared and kept at 34–36°C in artificial cerebrospinal fluid with 10 μM bicuculline free base [a concentration that has been shown to not measurably affect currents of Ca^{2+}-activated K^+ channels with small conductance (SK) or afterhyperpolarizations (AHPs) in rat brain slices (14, 15) and to cause only a ≈20% inhibition of SK channels expressed in frog oocytes (16)] and 10 μM 6,7-dinitroquinoxaline-2,3-dione (DNQX) to block synaptic transmission. Whole-cell (Axoclamp 2A, Axon Instruments, Union City, CA) and extracellular (Multiclamp 700A, Axon Instruments) recordings were obtained from PC somata under visual control. To compare the first action potential (AP) and AHP evoked by a depolarizing current pulse, a weak hyperpolarizing DC was injected to silence the cell before testing.

Recording of Inhibitory Synaptic Potentials in Deep Cerebellar Nuclei (DCN). Cerebellar slices from 13- to 17-day-old mice were prepared and superfused with artificial cerebral spinal fluid at room temperature. Whole-cell recordings (Axopatch 1-D) from large DCN neurons (Ø > 15 μm, hence presumably glutamatergic projecting neurons) in the lateral or medial nuclei, with 4 mM kynurenic acid blocking excitatory amino acid neurotransmission. PC axons were stimulated with a pair of tungsten microelectrodes, with different interstimulus intervals. Paired-pulse depression was quantified as the ratio between the average peak amplitudes of the responses to second and first stimuli.

Results

Generation of BK$^{-/-}$ Mice. The BK channel consists of four α subunits and four optional auxiliary β subunits (17). The pore-forming α subunit is encoded by only a single gene, KCNMA1 (also called *Slo*), from which multiple splice isoforms are generated (18, 19), whereas there are four different β subunit genes with tissue-specific expression (20–23). To determine BK channel functions, we generated mice lacking functional BK channels. The pore exon of the α subunit, which also encodes part of the S6 segment, was deleted through homologous recombination (Fig. 5). We obtained BK (*mSlo*) channel-deficient mice (BK$^{-/-}$) that completely lack the BKα mRNA and protein (Fig. 1 *a* and *b*). In the cerebellum, *in situ* hybridization experiments (Fig. 1*a*) indicate that mRNA encoding the BKα subunit is predominantly observed in PC somata, whereas only very low message levels are detected in the molecular layer, the granule cell layer, and the DCN, respectively. In clear contrast, BK channel protein (Fig. 1 *b* and *c*) is observed in PC somata, the molecular layer (where PC dendrites arborize), and the DCN (where PC axons project to). This finding suggests that the expression of BK channels in the cerebellum is predominantly, but not exclusively, in PCs where they are likely to be targeted to both the somato-dendritic and axonal compartments. Other principal neurons of the cerebellum express BK channels at levels considerably below that of PCs (24).

Macroscopic and microscopic analysis (Nissl staining) did not reveal any morphological abnormalities in young or adult BK$^{-/-}$ brains. The mutant mice had a normal life expectancy compared to their WT littermates but showed obvious ataxia. Furthermore, at 4 and 8 weeks of age, the BK$^{-/-}$ mice (males and females) showed 15–20% smaller body length and weight compared to their WT littermates, but the length and weight became normal at 12 weeks of age (Fig. 6, which is published as supporting information on the PNAS web site). The mutant mice also showed moderate vascular dysfunctions (≈10% increase in arterial blood pressure and changes in its regulation). These vascular effects, which were found to be due to BK channel deficiency in vascular smooth muscle and clearly unrelated to the neurological deficits, will be described elsewhere.

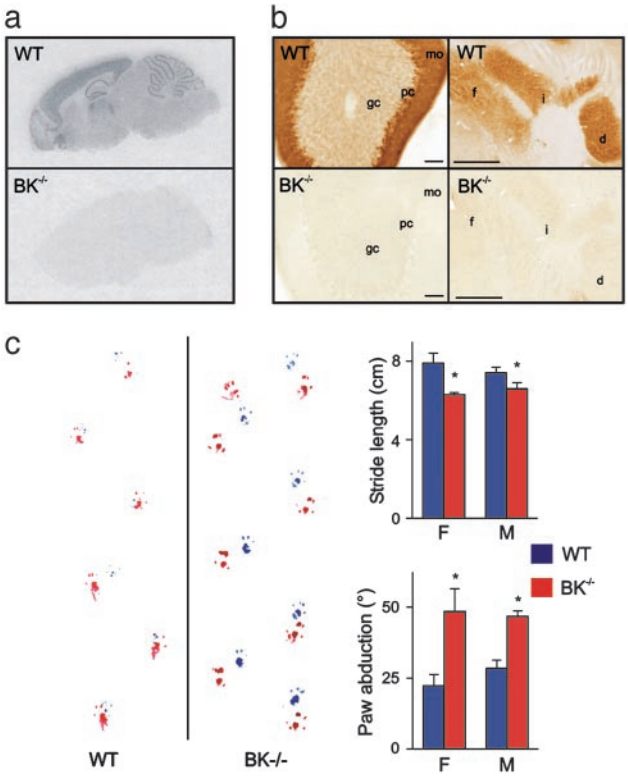

Fig. 1. Analysis of BK channel expression in brain and footprint pattern of WT and BK$^{-/-}$ mice. (*a*) Autoradiogram of brain sagittal sections from BK$^{+/+}$ and BK$^{-/-}$ mice hybridized *in situ* with BK channel α subunit probe. (*b*) Immunohistochemical detection of BK channels in mouse cerebellar coronal sections: dense BKα immunostaining in the molecular layer (mo), PC somata (pc), and DCN: fastigial (f), interpositus (i), dentate (d) nucleus; weak staining in granule cells (gc) layer. BK$^{-/-}$ sections incubated in parallel showed no staining. [Bars = 60 μm (on the left); 400 μm (on the right).] (*c*) Abnormal gait in BK$^{-/-}$ mice. Footprints of 4-month-old WT and BK$^{-/-}$ siblings (blue, forepaws; red, hindpaws). Statistics of stride length and paw abduction for males (M) and females (F). Three values were obtained from each run, excluding beginning and end; n = 6 WT and 7 BK$^{-/-}$ per gender.

Motor Impairment in BK$^{-/-}$ Mice. The BK$^{-/-}$ mice exhibited intention tremor and abnormal gait (12). Thus, the mutant mice showed shorter strides and irregular step pattern as compared with the WT mice (Fig. 1*c*). The angle between the left and right hindpaw axes was almost doubled, whereas the hindpaw width was similar between WT and mutants. These alterations were seen at all ages and in both genders.

The motor impairment precluded common tests of spatial learning such as the water maze. Thus, the mutants showed reduced swim speed and more frequent floating. To test motor coordination and balance, we used beam walking (12). The BK$^{-/-}$ mice were reluctant to traverse the beam (Fig. 2*a*), and, if trying, they made more slips and hindpaw errors and often fell off the beam or off the start platform, thus indicating severe motor impairment. In the accelerating rotarod test, which also requires good sensorimotor coordination and is sensitive to cerebellar and basal ganglia dysfunction (11), the BK$^{-/-}$ mice of both genders showed a strongly reduced latency to fall (Fig. 2*b*). Despite starting at a much lower level, the mutants improved at

PHYSIOLOGY

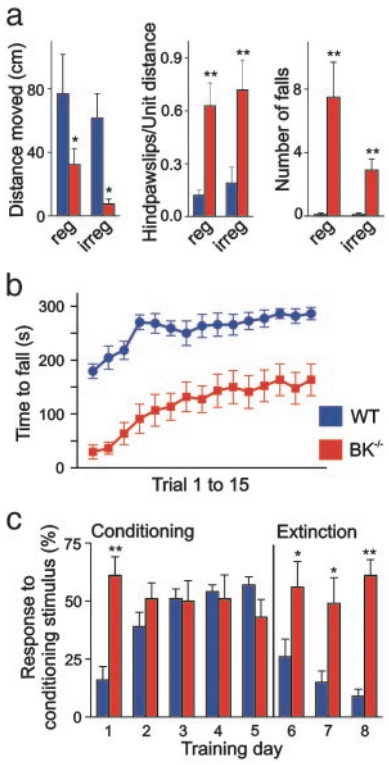

Fig. 2. Motor impairment and abnormal conditioned eye blinking in $BK^{-/-}$ mice. (*a*) Beam walking performance at regular (reg; i.e., smooth) beam and irregular (irreg; i.e., with steps) beam: distance moved, hindpaw slips, and falls. Means of two trials per beam, $n = 6$ per gender. (*b*) Accelerating rotarod performance: time to fall off the rotarod (mean value per trial), $n = 6$ per gender. (*c*) The conditioned eye-blink reflex, a cerebellum-specific form of motor learning, was abnormal in the $BK^{-/-}$ mice. Statistical summary of conditioned eye blinking results from eight WT and eight $BK^{-/-}$ mice. The conditioning phase includes 5 days followed by 3 days for extinction. All data are means ± SEM, *, $P < 0.05$; **, $P < 0.01$.

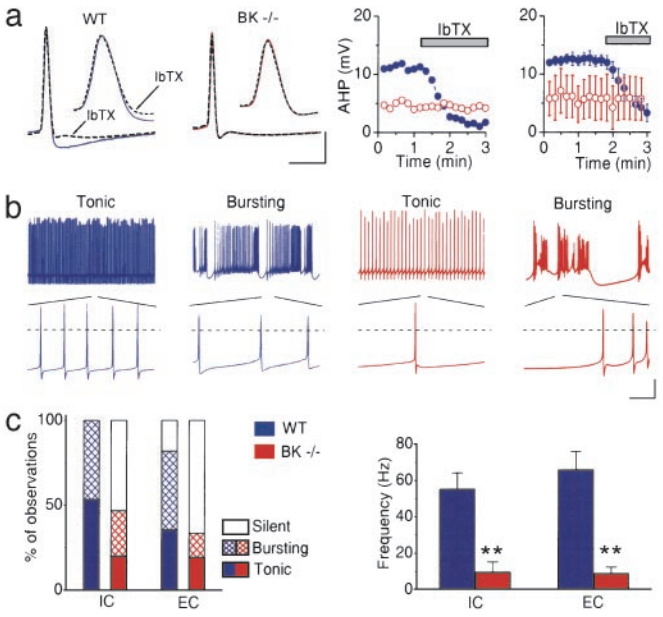

Fig. 3. Reduction of fast AHP and severely reduced firing activity in $BK^{-/-}$ PCs. (*a Left*) Effects of BK-channel blockade by IbTx (1 μM) on AHP and AP (*Insets*) in WT (blue) and $BK^{-/-}$ (red) PCs. Records were obtained before (continuous trace) and 1 min after IbTx application (dashed). [Bars = 2 ms/20 mV (AHPs), 0.5 ms/30 mV (APs)]. (*Center*) Time courses of IbTx effects on AHP in WT and $BK^{-/-}$ PCs yielding the sample traces. (*Right*) Average time course of the AHP amplitudes of $n = 5$ WT and 3 $BK^{-/-}$ PCs. (*b*) Whole-cell [intracellular (IC)] recordings from WT and $BK^{-/-}$ PCs, showing spontaneous tonic and bursting firing patterns at fast and slow time scales. (Dashed lines, AP detection threshold for interspike interval distributions in Fig. 4*a*). (Bars = 200 ms/20 mV, 10 ms/20 mV.) (*c*) Distribution of trimodal firing patterns and difference in overall average firing rate between WT and $BK^{-/-}$ PCs for whole-cell (IC) and cell-attached [extracellular (EC)] recordings, for the first 2 min of recording; $n = 14$–22 PCs per condition and genotype.

a rate similar to the WT (Fig. 2*b*), indicating that they partially compensated their deficit through motor learning. The $BK^{-/-}$ mice showed motor impairment also in the open field test: reduced distance, path linearity, and exploration index, as well as lack of typical acceleration when leaving the center field (data not shown).

Abnormal Eye-Blink Reflex in $BK^{-/-}$ Mice. The motor impairment prompted us to examine cerebellar function. The cerebellum adjusts the operation of motor centers in the cortex and brainstem during movements and is needed for balance, precision timing, and sensorimotor learning, functions that appeared to be affected in the mutants. To test cerebellar function, we adopted the conditioned eye-blink response, a well established behavioral test of cerebellar learning (13). An air puff to the eye elicits the eye-blink reflex, the unconditioned response. After repeated pairing of a tone and the air puff, the tone alone evokes a conditioned blinking response, via one of the DCN, the interpositus nucleus. Before conditioning, tone-induced impulses are blocked at this nucleus by the inhibitory input from cerebellar PCs. When combined, the two inputs converge on the PCs, the tone via parallel fibers, and the air puff via climbing fibers, and induce long-term depression of the parallel fiber/PC synapses, thereby reducing PC activity and, hence, PC inhibition of the interpositus neurons (13).

When tested with repeatedly paired tone and air puff, the WT mice learned conditioned eye blinking rapidly (Fig. 2*c*). In contrast, the $BK^{-/-}$ mice showed no learning of the conditioned eye blink. Instead, they showed increased eye blinking up to the highest level observed in trained WT mice, suggesting maximal disinhibition of the interpositus nucleus. These results support the hypothesis of cerebellar dysfunction in the $BK^{-/-}$ mice.

Depolarization Block of Cerebellar PC. To search for a possible cellular basis of cerebellar dysfunction in the $BK^{-/-}$ mice, we recorded the firing activity of PCs. We focused on this cell type because projections from these cells to the DCN are the only output from the cerebellar cortex. Because BK channels may be involved in AP repolarization and fast AHPs (25, 26), we compared AP waveforms and AHPs in cerebellar slices. To suppress spontaneous discharge and ensure comparable recording conditions, we maintained the pretest membrane potential at a constant level (−60 to −70 mV) by direct current injection, and evoked APs by depolarizing current pulses. In PCs from WT mice, the BK channel blocker iberiotoxin (IbTx, 1 μM) (1) strongly suppressed the single-spike AHP and slowed AP repolarization (Fig. 3*a*). In contrast, IbTx had no measurable effect on AHPs or APs in PCs from $BK^{-/-}$ mice. Furthermore, the AHP amplitude was significantly smaller in $BK^{-/-}$ (4.5 ± 0.8 mV, $n = 14$) vs. WT neurons (10.1 ± 1.8mV, $n = 13$; $P < 0.01$). The mean AP 90–10% decay time was slightly but not significantly longer in $BK^{-/-}$ cells (0.27 ± 0.09 ms, $n = 5$, vs. 0.21 ± 0.01 ms in WT, $n = 5$), suggesting that there may be compensatory changes in other repolarizing mechanisms, or that the difference was too small to be detected statistically. Taken together, these observations suggest that the main role of BK

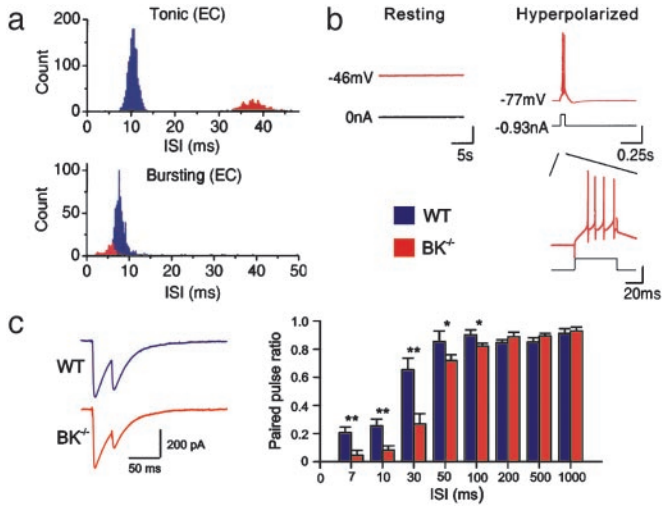

Fig. 4. Spontanous discharge rates and depolarization block of $BK^{-/-}$ cerebellar PC and increased depression at their DCN synapses. (*a*) Interspike interval (ISI) distributions for four typical PCs: tonic-firing (*Upper*) and burst-firing (*Lower*) WT and $BK^{-/-}$ PCs. In each case, total AP number during a 15-s period is plotted. Note the fewer APs in $BK^{-/-}$ compared with WT PCs, and longer ISI (lower discharge rate) in tonic-firing $BK^{-/-}$ PCs. (*b*) Whole-cell recording from a silent $BK^{-/-}$ PC with a depolarized resting potential (−46 mV). APs were evoked by hyperpolarizing the cell to −77 mV with DC current (−0.93 nA) before a depolarizing pulse (1.2 nA, 50 ms). (Bar = 20 mV, 1.7 nA.) (*c*) Enhanced paired-pulse depression in PC-DCN synapses. Significant differences were found for intervals shorter than 100 ms, $n = 6$ per genotype. (*Left*) Inhibitory postsynaptic currents (averages of 15 consecutive recordings) evoked by paired pulses (30-ms interval) in WT and $BK^{-/-}$ slices. All data are means ± SEM, **, $P < 0.01$; *, $P < 0.05$.

channels in PCs is to generate AHPs (26), with only a modest effect on the AP itself (Fig. 3*a*).

Normal PCs fire spontaneous APs under basal conditions, thereby tonically inhibiting the DCN (27). Surprisingly, >50% of the PCs from $BK^{-/-}$ mice lacked spontaneous discharge (8 of 15 cells, 53.3%), in sharp contrast to the WT cells, which all generated spontaneous APs during whole-cell recording (15 of 15 cells; Fig. 3*c Left*). Thus, the overall discharge activity was abnormally low in mutant PCs. The average spike frequency for all cells was ≈6-fold higher in WT cells (55.2 ± 8.9 Hz) than in $BK^{-/-}$ cells (9.5 ± 5.6 Hz; $P < 0.01$) (Fig. 3*c Right*). PCs from both WT and $BK^{-/-}$ mice showed two distinct spontaneous firing patterns (28, 29): tonic-firing PCs vs. repetitive bursting PCs (Fig. 3*b*) and the proportions of these were not statistically different between $BK^{-/-}$ (20.0% tonic, 26.7% bursting) and WT mice (53.3% tonic, 46.7% bursting) (Fig. 3*c Left*).

To avoid possible artifacts due to dialysis via the recording pipette, we also performed somatic loose-patch extracellular recordings from PCs (30). Again, the overall spontaneous firing rate was far lower in the $BK^{-/-}$ (8.7 ± 3.6 Hz) than in the WT cells (65.7 ± 10.1 Hz), mainly due to more silent cells (Fig. 3*c Right*). In addition, among the tonic-firing PCs, the $BK^{-/-}$ cells showed longer interspike intervals (Fig. 4*a Top*) and hence lower discharge frequency (37.1 ± 7.2 Hz, $n = 4$) than WT cells (91.6 ± 15.8 Hz, $n = 8$; $P < 0.01$; not shown). The frequency distributions and cumulative frequency plots of the spontaneous firing rates also showed highly significant differences between $BK^{-/-}$ and WT cells, for both whole-cell and loose-patch recordings. In both cases, the $BK^{-/-}$ PC firing was skewed toward frequencies <20 Hz (Fig. 7, which is published as supporting information on the PNAS web site). Taken together, PCs from mice lacking BK channels showed an abnormally reduced spontaneous discharge activity.

Why were these mutant PCs silent? The whole-cell data showed that the resting membrane potential of the silent cells stayed at a depolarized level (−45 to −50 mV; Fig. 4*b Left*). In most cases it was constant, but some (two of eight) cells showed slow shallow oscillations (0.2–0.5 Hz, 15- to 20-mV amplitude; not shown). Depolarizing current injections in silent mutant cells failed to evoke APs. However, after being hyperpolarized to −70 or −80 mV by current injection, each of these silent $BK^{-/-}$ cells could fire normal fast APs (Fig. 4*b Right*), indicating that their silence was caused by depolarization block, i.e., inactivation of their Na^+ channels (31). Current-voltage (I/V) plots (V measured near the end of 500-ms-long injected current pulses) were nearly identical (<1-mV difference) for $BK^{-/-}$ ($n = 11$) and WT ($n = 9$) PCs at potentials <−70mV, whereas at >−65 mV, the mutant PCs showed on average 2- to 5-mV larger subthreshold depolarizations than WT cells. Although this difference was not statistically significant, it may possibly reflect a change in subthreshold currents (Fig. 8, which is published as supporting information on the PNAS web site).

As expected, IbTx had no effects in mutant PCs. In the tonic WT cells, IbTx increased the discharge frequency (26) and, in some PCs, eventually precipitated a transition into bursting mode. In bursting WT cells, IbTx induced complex changes in the burst patterns (not shown). However, neither tonic nor bursting WT cells became steadily depolarized or silent during the recordings in IbTx (lasting 15–45 min). Whatever the mechanism, the lack of BK channels evidently reduced the PC basal discharge activity to only a fraction of the normal level (Fig. 3*c*).

Increased Short-Term Depression at the PC/DCN Synapses. The results so far suggest that dramatic reduction of PC activity leads to a disinhibition of DCN. To assess the inhibitory effect of the impulses that were still generated in PCs, we performed whole-cell recordings from DCN neurons from $BK^{-/-}$ and WT mice. Stimulation of PC axons (while excitatory receptors were blocked) evoked inhibitory postsynaptic currents (IPSCs) that could be blocked by $GABA_AR$ antagonists. The IPSCs in WT and $BK^{-/-}$ DCNs had similar rise times, half widths, and amplitudes, without any significant difference between the two genotypes (Fig. 9, which is published as supporting information on the PNAS web site).

If BK channels contribute to presynaptic APs or AHPs, differences in neurotransmitter release might become evident during high-frequency activation, corresponding to the high firing frequencies of PCs *in vivo*. Therefore, we used paired stimulation to test the frequency dependence of transmission at the PC/DCN synapses. As illustrated in Fig. 4*c*, the paired-pulse depression, which is also seen in normal PCs (32), was significantly increased in DCNs from $BK^{-/-}$ mice, but only for intervals shorter than 100 ms. Thus, BK channels apparently regulate high-frequency synaptic transmission. Possibly, the absence of BK channels impaired repolarization and/or AHP after the first spike, thus causing incomplete deinactivation of Na^+ channels, reducing the subsequent spike amplitude and Ca^{2+} influx, thereby causing synaptic depression. Taken together, the attenuated transmission at PC/DCN synapses and the reduced activity of PCs are expected to synergistically diminish the GABAergic outflow from the cerebellar cortex, thus causing disinhibition of the DCN which, in turn, may explain the observed motor deficits.

Discussion

Deletion of the BK channel α subunit in mice permitted the first identification of the physiological functions of this unique channel type in a vertebrate species *in vivo* and revealed unexpected roles of BK channels in cerebellar function. The consequences of BK channel ablation exceed by far those caused by deletion of

the regulatory BK channel β_1 subunit, which is not significantly expressed in neurons and produced no neural effects (33, 34). Nevertheless, the BK channels, despite their widespread expression in the CNS (24), appear to play surprisingly modest roles in normal brain function. This suggests that their wide neuronal expression has evolved partly because BK channels are more important under stress and deleterious conditions, a view supported by the observation that BK channels improve the survival of neurons exposed to ischemic conditions (35).

A principal finding of this study is that the mice lacking BK channels showed apparent loss of eye-blink conditioning. This learning behavior depends on the cerebellar circuitry and not on the basal ganglia or cerebral motor cortex (36). The naive $BK^{-/-}$ mice showed already from the first training session an abnormally high blinking rate, suggesting a profound disinhibition of the DCN. This could be caused by the observed severe suppression of spontaneous PC activity, combined with the increased short-term depression at the inhibitory PC/DCN synapses. Although evaluation of eye-blink learning is not possible when the blinking rate is already close to maximal in the training phase, this impairment suggests cerebellar dysfunction. Hence the motor learning of $BK^{-/-}$ mice on the rotarod may involve mainly noncerebellar functions, e.g., corticostriatal plasticity (37).

The severe suppression of PC activity and synapses observed in the $BK^{-/-}$ mice is therefore a likely cause of their motor coordination deficits and ataxia. PCs are essential for cerebellar motor control (38–40) by providing specific timing signals for movement coordination (41). BK channels in PCs are activated by depolarization and Ca^{2+} influx, via opening of P/Q type Ca^{2+} channels during APs (26, 31) and contribute to AP repolarization and AHPs. The depolarization block caused by the BK channel deletion suggests that the net effect of P/Q channel activation is to polarize the membrane via activation of BK channels, thus maintaining normal excitability (31). The failure of IbTx applications in WT slices to mimic the depolarization block found in mutants may be due to incomplete block of toxin-resistant BK channels (21), or perhaps longer-lasting suppression of BK channels is needed to induce the silent state, possibly by inducing compensatory changes in other membrane conductances. Interestingly, loss of P/Q channel function, due to various mutations, can cause cerebellar ataxia in humans (42). Our results suggest that these forms of inherited cerebellar ataxia may be partly due to lack of BK channel activation. Thus, the $BK^{-/-}$ mice, which represent a previously undescribed animal model of cerebellar ataxia, may prove useful for understanding normal and pathological cerebellar function, and studies of BK channel-dependent functions *in vivo* are likely to help clarify the therapeutic utility of BK channel activators or blockers (9).

We thank the Deutsche Forschungsgemeinschaft, Fonds zur Förderung der Wissenschaftlichen Forschung, the Research Council of Norway, Wellcome Trust, the National Centre of Competence in Research, the Thyssen-Stiftung, and the Schilling Foundation for support.

1. Hille, B. (2001) in *Ion Channels of Excitable Membranes* (Sinauer, Sunderland, MA), pp. 131–168.
2. Cooper, E. C. & Jan, L. Y. (1999) *Proc. Natl. Acad. Sci. USA* **96,** 4759–4766.
3. Browne, D. L., Gancher, S. T., Nutt, J. G., Brunt, E. R., Smith, E. A., Kramer, P. & Litt, M. (1994) *Nat. Genet.* **8,** 136–140.
4. Herson, P. S. (2003) *Nat. Neurosci.* **6,** 378–383.
5. Singh, N. A., Charlier, C., Stauffer, D., DuPont, B.R., Leach, R. J., Melis, R., Ronen, G. M., Bjerre, I., Quattlebaum, T., Murphy, J. V., *et al.* (1998) *Nat. Genet.* **18,** 25–29.
6. Surmeier, D. J., Mermelstein, P. G. & Goldowitz, D. (1996) *Proc. Natl. Acad. Sci. USA* **93,** 11191–11195.
7. Curran, M. E. (1998) *Curr. Opin. Biotechnol.* **9,** 565–572.
8. Latorre, R., Oberhauser, A., Labarca, P. & Alvarez, O. (1989) *Annu. Rev. Physiol.* **51,** 385–399.
9. Gribkoff, V. K., Starrett, J. E. & Dworetzky, S. I. (2001) *Neuroscientist* **7,** 66–177.
10. Calderone, V. (2002) *Curr. Med. Chem.* **9,** 1385–1395.
11. Crawley, J. N. (1999) *Brain Res.* **835,** 18–26.
12. Carter, R. J., Lione, L. A., Humby, T., Mangiarini, L., Mahal, A., Bates, G. P., Dunnett, S. B. & Morton, A. J. (1999) *J. Neurosci.* **19,** 3248–3257.
13. Linden, D. J. (2003) *Science* **301,** 1682–1685.
14. Debarbieux, F., Brunton, J. & Charpak, S. (1998) *J. Neurophysiol.* **79,** 2911–2918.
15. Seutin, V. & Johnson, S. W. (1999) *Trends Pharmacol. Sci.* **20,** 268–270.
16. Khawaled, R., Bruening-Wright, A., Adelman, J. P. & Maylie, J. (1999) *Pflügers Arch.* **438,** 314–321.
17. Orio, P., Rojas, P., Ferreira, G. & Latorre, R. (2002) *News Physiol. Sci.* **17,** 156–161.
18. Butler, A., Tsunoda, S., McCobb, D. P., Wei, A. & Salkoff, L. (1993) *Science* **261,** 221–224.
19. Tseng-Crank, J., Foster, C. D., Krause, J. D., Mertz, R., Godinot, N., DiChiara, T. J. & Reinhart, P. H. (1994) *Neuron* **13,** 1315–1330.
20. Knaus, H.-G., Garcia-Calvo, M., Kaczorowski, G. J. & Garcia, M. L. (1994) *J. Biol. Chem.* **269,** 3921–3924.
21. Wallner, M., Meera, P. & Toro, L. (1999) *Proc. Natl. Acad. Sci. USA* **96,** 4137–4142.
22. Brenner, R., Jegla, T. J., Wickenden, A., Liu, Y. & Aldrich, R. W. (2000) *J. Biol. Chem.* **275,** 6453–6461.
23. Meera, P., Wallner, M. & Toro, L. (2000) *Proc. Natl. Acad. Sci. USA* **97,** 5562–5567.
24. Knaus, H.-G., Schwarzer, C., Koch, R. O., Eberhart, A., Kaczorowski, G. J., Glossmann, H., Wunder, F., Pongs, O., Garcia, M. L. & Sperk, G. (1996) *J. Neurosci.* **16,** 955–963.
25. Storm, J. F. (1987) *J. Physiol.* **385,** 733–759.
26. Edgerton, J. R. & Reinhart, P. H. (2003) *J. Physiol.* **548,** 53–69.
27. Llinas, R. R. & Walton, K. D. (1998) in *The Synaptic Organization of the Brain*, ed. Shepherd, G. M. (Oxford Univ. Press, New York), pp. 255–288.
28. Cingolani, L. A., Gymnopoulos, M., Boccaccia, A., Stocker, M. & Pedarzani, P. (2002) *J. Neurosci.* **22,** 4456–4467.
29. Womack, M. & Khodakhah, K. (2002) *J. Neurosci.* **22,** 10603–10612.
30. Häusser, M. & Clark, B. A. (1997) *Neuron* **19,** 665–678.
31. Raman, I. M. & Bean, B. P. (1999) *J. Neurosci.* **19,** 1663–1674.
32. Pedroarena, C. M. & Schwarz, C. (2003) *J. Neurophysiol.* **89,** 704–715.
33. Plüger, S., Faulhaber, J., Fürstenau, M., Löhn, M., Waldschütz, R., Gollasch, M., Haller, H., Luft, F. C., Ehmke, H. & Pongs, O. (2000) *Circ. Res.* **87,** E53–E60.
34. Brenner, R., Perez, G. J., Bonev, A. D., Eckman, D. M., Kosek, J. C., Wiler, S. W., Patterson, A. J., Nelson, M. T. & Aldrich, R. W. (2000) *Nature* **407,** 870–876.
35. Runden-Pran, E., Haug, F. M., Storm, J. F. & Ottersen, O. P. (2002) *Neuroscience* **112,** 277–288.
36. Bracha, V. (2004) *Prog. Brain Res.* **143,** 331–339.
37. Kelley, A. E., Andrzejewski, M. E., Baldwin, A. E., Hernandez, P. J. & Pratt, W. E. (2003) *Ann. N.Y. Acad. Sci.* **1003,** 159–168.
38. Thach, W.T. & Bastian, A. J. (2004) *Prog. Brain Res.* **143,** 353–366.
39. Bloedel, J. R. (2004) *Prog. Brain Res.* **143,** 319–329.
40. Nolan, M. F., Malleret, G., Lee, K. H., Gibbs, E., Dudman, J. T., Santoro, B., Yin, D., Thompson, R. F., Siegelbaum, S. A., Kandel, E. R., Morozov, A., *et al.* (2003) *Cell* **115,** 551–564.
41. Jaeger, D. & Bower, J. M. (1999) *J. Neurosci.* **19,** 6090–6101.
42. Zhuchenko, O., Bailey, J., Bonnen, P., Ashizawa, T., Stockton, D. W., Amos, C., Dobyns, W. B., Subramony, S. H., Zoghbi, H. Y. & Lee, C. C. (1997) *Nat. Genet.* **15,** 62–69.